MPMI Vol. 19, No. 6, 2006, pp. 577–587. DOI: 10.1094/MPMI-19-0577. © 2006 The American Phytopathological Society

Arabidopsis Displays Centromeric DNA Hypomethylation and Cytological Alterations of Heterochromatin Upon Attack by *Pseudomonas syringae*

Valeria Pavet,[1] Cristián Quintero,[1] Nicolás M. Cecchini,[1] Alberto L. Rosa,[2] and María E. Alvarez[1]

[1]CIQUIBIC—Departamento de Química Biológica, Facultad de Ciencias Químicas, Universidad Nacional de Córdoba, 5000 Córdoba, Argentina; [2]Instituto de Investigación Médica Mercedes y Martín Ferreyra—INIMEC, Friuli 2434, 5016 Córdoba, Argentina

Submitted 12 September 2005. Accepted 25 January 2006.

Plant tissues display major alterations upon the perception of microbial pathogens. Changes of cytoplasmic and apoplastic components that sense and transduce plant defenses have been extensively characterized. In contrast, less information is available about modifications affecting the plant nuclear genome under these circumstances. Here, we investigated whether the *Arabidopsis thaliana* DNA methylation status is altered in tissues responding to the attack of *Pseudomonas syringae* pv. *tomato* DC3000. We applied amplified fragment length polymorphism analysis to monitor cytosine methylation at anonymous 5′-CCGG-3′ and 5′-GATC-3′ sites in naïve and infected samples. Plant genomic fragments reducing methylation upon infection, including peri/centromeric repeats such as the 180-bp unit, *Athila* retrotansposon, and a portion of the nuclear insertion of mitochondrial DNA, were isolated and characterized. *P. syringae* pv. *tomato*-induced hypomethylation was detected by high-performance liquid chromatography assays and at the molecular level it did not seem to equally affect all 5-methyl cytosine (5-mC) residues. Nuclei from challenged tissues displayed structural chromatin alterations, including loosening of chromocenters, which also were stimulated by avirulent *P. syringae* pv. *tomato,* but not by the *P. syringae* pv. *tomato hrpL*⁻ mutant. Finally, *P. syringae* pv. *tomato*-induced hypomethylation was found to occur in the absence of DNA replication, suggesting that it involves an active demethylation mechanism. All these responses occurred at 1 day postinfection, largely preceding massive plant cell death generated by pathogen attack.

Additional keywords: biotic stress, DNA methylation changes, interphase nuclei.

The most common DNA modification of animal and plant genomes is the incorporation of a methyl group in the carbon 5 of the pyrimidine ring of cytosine (C) generating 5-mC (5-methyl cytosine). Plant genomes concentrate DNA methylation in repetitive noncoding sequences and in transposons where 5-mC residues are found in symmetric (CpG, CpYpG; Y: A, T, C) and asymmetric (CpYpY) sites (Martienssen and Colot 2001). In addition, clusters of dense CG methylation are detected mainly in genes (Tran et al. 2005). Patterns of C methyllation constitute epigenetic marks which can be either maintained or modified by de novo methylation or demethylation. In plants, de novo DNA methylation is activated upon the introduction of foreign sequences into the genome (Matzke et al. 2000), whereas demethylation may result from "passive" or "active" processes. Perpetuation of methylation marks at symmetric sites over DNA replication requires the activity of maintenance DNA methyltransferases that use hemimethylated DNA strands as a guide for remethylation of newly synthesized daughter strands. In the absence of this enzymatic activity, passive DNA demethylation takes place (Bird 2002). In contrast, active DNA demethylation involves enzymatic mechanisms removing the methylated residues under nonreplicative conditions. Although several reports suggested the occurrence of active demethylation in plants and animals, evidence for such enzymatic activity in vivo is still limited (Bhattachayra et al. 1999; Bird 2002; Cui and Fedoroff 2002; Gong et al. 2002; Weiss et al. 1996).

At the functional level, DNA methylation is implicated in maintenance of chromatin structure and epigenetic states (Martienssen and Richards 1995), control of plant development (Finnegan et al. 1996; Kakutani et al. 1996; Ronemus et al. 1996), transition into reproductive phase (Soppe et al. 2000), silencing of foreign genes (Matzke et al. 2000), genomic imprinting, and avoidance of homologous recombination (Bender 2004). In addition, it is likely that de novo DNA methylation plays a primary role as a component of nuclear defensive mechanisms preserving the genome integrity by preventing transposons mobility and post-transcriptional gene silencing and by repressing viral gene expression (Matzke et al. 2000; Yoder et al. 1997).

Plants, unlike mammals, can transmit DNA methylation changes between generations. After fertilization, plant genomes apparently do not support a wave of DNA demethylation. In addition, low activity of de novo DNA methyltransferases is detected in plants. Hypomethylated single-copy genes and repetitive sequences of transgenic (Ronemus et al. 1996) or mutant (Vongs et al. 1993) *Arabidopsis* plants do not become remethylated upon meiosis, not even when the mutation causing the methylation defect is segregated in sexual crosses (Finnegan et al. 1996; Kakutani et al. 1999; Ronemus et al. 1996; Saze et al. 2003). In addition, *Arabidopsis* domains rearranged methylase (drm) mutants impaired in de novo DNA methylation do not reduce their preexisting DNA methylation levels after inbreeding (Cao and Jacobsen 2002). On the other hand, massive DNA demethylation (approximately 70%) can generate heritable lesions causing plant developmental abnormalities (Kakutani et al. 1996; Ronemus et al. 1996 Vongs et al. 1993) and can even result in early embryonic lethality (Saze et al. 2003).

Corresponding author: María E. Alvarez;
E-mail: malena@mail.fcq.unc.edu.ar

Previous evidence suggested that plant DNA methylation can be altered under abiotic and biotic stress conditions. Cold-treatment leads to reduction of 5-mC in the genome of tobacco cultured cells (Burn et al. 1993), *Arabidopsis* seedlings (Finnegan et al. 1998), and maize root tissues (Steward et al. 2002). Viroids infection directs de novo methylation of homologous DNA sequences that have been integrated into the plant genome (Wassenegger et al. 1994). Conversely, *Tobacco mosaic virus* infection induces hypomethylation of tobacco genomic regions such as the pathogen-responsive *NtAlix1* gene, which becomes concomitantly activated (Wada et al. 2004). Concerning infections caused by extracellular pathogens, altered plant DNA methylation has been reported for the cotton–*Verticillium* spp. pathosystem, but only at the biochemical level (Guseinov and Vanyushin 1975). Changes in other host chromatin remodeling factors intimately related to DNA methylation were characterized in more detail in other systems. Fungal infections were found to produce enhancement of acetylated histones in maize (Brosch et al. 1995) and *Arabidopsis* (Zhou et al. 2005). The HC toxin from *Cochliobolus carbonum* was shown to inhibit plant histone deacetylases (HDAC) in susceptible cultivars, and this toxin could be detoxified by a host carbonyl reductase encoded by the *Hm1* gene, which was present in maize resistant cultivars (Johal and Briggs 1992). In *Arabidopsis*, downregulation of the gene encoding HDAC19 increased the host histone acetyation levels, exacerbating plant susceptibility to infections by *Alternaria brassicicola* (Zhou et al. 2005).

We evaluated whether the genomic methylation status of *Arabidopsis thaliana* could be modified upon infection by *Pseudomonas syringae* pv. *tomato* DC3000. The attack of this virulent bacterial strain stimulates weak or transient host defenses which are insufficient to control pathogen proliferation. Consequently, bacterial clusters accumulate into mesophyll intercellular spaces, generating chlorotic and water soaked lesions (Whalen et al. 1991). Net changes of the *A. thaliana* transcriptome take place during the initial 9 h of *P. syringae* pv. *tomato* attack, and this response was found to be qualitatively similar but of lower intensity than that activated upon perception of isogenic avirulent bacteria (Tao et al. 2003). Here, we describe how tissues infected with either virulent *P. syringae* pv. *tomato* producing disease or the isogenic avirulent strain, *P. syringae* pv. *tomato-avrRpt2*, triggering *R*-gene-dependent defenses, display alterations in their DNA methylation status at 24 h postinfection (hpi). Cytosine methylation patterns are modified and overall 5-mC content is reduced in infected tissues. Three peri/centromeric loci that show DNA hypomethylation were identified and modifications affecting the centromeric heterochromatin structure under this infection condition were characterized.

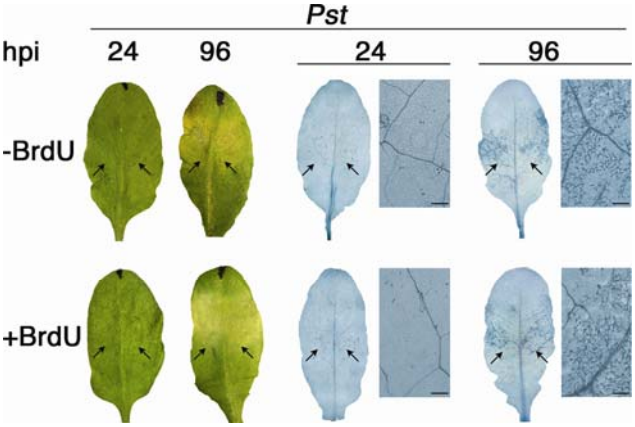

Fig. 1. Disease features produced by localized infiltration of virulent *Pseudomonas syringae* pv. *tomato* (*Pst*) (10^6 CFU/ml) into adult *Arabidopsis thaliana* leaf tissues. Infiltration sites are indicated by arrows. Symptoms were monitored at the indicated hours postinfiltration (hpi). Lactophenol trypan blue staining was used to visualize plant cell death. At the macroscopic level, chlorotic lesions and massive cell death were not detected at 24 hpi but clearly evidenced at 96 hpi. Plants either untreated (–BrdU) or fed with 150 μM 5-bromo-2′-deoxyuridine (+BrdU) and further infiltrated with *P. syringae* pv. *tomato* displayed similar responses. Magnifications correspond to microscopic images of infiltration sites. Bars: 100 μM.

RESULTS

The *A. thaliana* genome modifies its methylation status upon infection by *P. syringae* pv. *tomato*.

When leaves from *A. thaliana* Col-0 plants were infiltrated with a moderate titer of *P. syringae* pv. *tomato* DC3000 (10^6 CFU/ml), clear disease symptoms and strong cellular collapse were evidenced at 4 days postinfiltration (dpi) (Fig. 1). In contrast, neither macroscopic signs of disease nor massive cell death were detected at 24 hpi in infected tissues (Fig. 1). We evaluated whether the plant DNA methylation status becomes modified in the *P. syringae* pv. *tomato*-treated tissues at 24 hpi. For that purpose, genomic DNA was isolated from naïve and infected leaves and analyzed by amplified fragment length polymorphism (AFLP) assays (Fig. 2A). AFLP assays previously were applied to study DNA methylation in *Arabidopsis*, revealing that genotypically identical plants have stable methylation at 5′-CCGG-3′ sites (Cervera et al. 2002). Unlike other AFLP systems (Cervera et al. 2002), our assay included digestion of DNA with two methylation-sensitive restriction enzymes, *Sau*3AI (5′-GATC-3′) and *Hpa*II (5′-CCGG-3′) (Fig. 2A), allowing us to monitor all plant DNA methylation contexts (CpG, CpYpG, and CpYpY). Seven DNA samples obtained from naïve, mock- (6, 24, and 72 hpi) and *P. syringae* pv. *tomato*-treated tissues (10^6 CFU/ml; 6, 24, and 72 hpi) were processed in parallel in each experiment. Similar electrophoretic profiles were obtained for samples corresponding to naïve and mock-inoculated tissues, indicating that basal methylation states of *Sau*3AI and *Hpa*II sites were homogeneous and were not significantly altered by the infiltration stress. Comparison of the seven samples revealed a few polymorphisms between naïve or mock-inoculated and pathogen-inoculated samples. An example of polymorphisms between mock- and *P. syringae* pv. *tomato*-inoculated samples isolated at 24 hpi is shown in Figure 2B. Polymorphic bands were purified from gels, reamplified by polymerase chain reaction (PCR), and further characterized (discussed below). After cloning and sequencing some of these products, we observed that DNA fragments corresponding to bands 3, 8, 9, 10, 20, 23, and 24 contained i) 5′ and 3′ sequences from the PCR primers, ii) the sequence of the radiolabeled primer used for the second PCR, and iii) nonchimeric genomic sequences containing or not containing internal *Sau*3AI or *Hpa*II sites. Hence, these clones were considered to be putative products of differential DNA methylation. Sequence analysis indicated that clones 8 and 24 harbored the 180-bp unit repeat (Fig. 2C), the highest abundant repeat in the *A. thaliana* genome located within the five centromeric domains (The Arabidopsis Genome Initiative 2000). Clones 3 and 9 contained two different fragments of a portion of mitochondrial DNA (mtDNA) located in BAC T17H1, whereas clones 10, 20, and 23 corresponded to single-copy genes located in BACs T12H1, K1F13, or F11I11, respectively (not shown).

P. syringae pv. *tomato* induces hypomethylation of plant centromeric loci.

The AFLP assay predicted neither whether polymorphic bands were originated by increase or decrease in DNA methylation, nor at which restriction sites (*Sau*3AI, *Hpa*II, or both) methylation was altered under infection. These features were ana-

lyzed by Southern blot experiments. DNA isolated from naïve and *P. syringae* pv. *tomato*-infected tissues (24 hpi) was digested with *Sau*3AI or *Hpa*II enzymes and further hybridized with probes from the AFLP polymorphic bands 8 (180-bp repetitive unit) and 3 (mtDNA). Considering that *Hpa*II is sensitive to methylation at both Cs of the site 5′-CCGG-3′, digestion with its isosquizomer *Msp*I (only sensitive to methylation of the outer C) was included to improve the methylation analysis. In addition, hypomethylated DNA from naïve *ddm1* plants (Vongs et al. 1993) was used as a control. *Sau*3AI digestions indicated that, in the infected samples, the low molecular weight bands increased at the expense of high molecular weight bands (Fig. 3A). For the 180-bp repeat, bands smaller than 1 kb concentrated 51% of the hybridization signal in wild-type naïve samples, whereas they retained 66 or 76% of the signal in samples treated with 10^6 or 5×10^6 CFU/ml of *P. syringae* pv. *tomato* (24 hpi), respectively. This response, indicative of reduction of 5-mCs from 5′-GATC-3′ sites of the 180-bp repeat, was stronger in leaves treated with higher doses of bacteria. However, *P. syringae* pv. *tomato* treatment induced lower hypomethylation at these sites than the *ddm1* mutation (Fig. 3A). Hybridization of the same blots with probes from the *RPS2* gene or 208 AFLP clone was used to confirm equal loading and digestion of DNA samples because these genomic fragments were insensitive to methylation changes upon infection (not shown).

*Hpa*II and *Msp*I digestions (5′-CCGG-3′ site) did not reveal variations in the methylation status of the 180-bp repeats in the infected tissues (Fig. 3A). This indicated that neither substantial loss of both 5-mCs together (*Hpa*II digestion), nor massive reduction of the external 5-mC of the site (*Msp*I digestion), occurred upon infection. Considering the latter result, and the fact that *Hpa*II is sensitive to methylation at both cytosines, changes affecting only the internal cytosine (CpG context) could not be evaluated.

We further analyzed methylation of the mtDNA sequences harbored in clone 3 and found hypomethylation of *Sau*3AI sites in the *P. syringae* pv. *tomato*-infected samples (Fig. 3B). Interestingly, these mtDNA sequences were found to be a target of *ddm1*-induced hypomethylation, and similar methylation levels were detected in *P. syringae* pv. *tomato*-infected samples and *ddm1* plants (Fig. 3B). We finally hybridized Southern blots with a probe from a third centromeric locus, the *Athila* retrotransposon. Once again, hypomethylation at *Sau*3AI sites was observed in the infected tissues (Fig. 3B). In contrast, methylation changes were not detected with *Hpa*II or *Msp*I for the mtDNA or *Athila* probes in *P. syringae* pv. *tomato*-treated tissues (not shown). Analysis of mock-inoculated samples by either Southern blot (Fig. 3A) or bisulfite (Fig. 3C) experiments indicated that DNA demethylation was not stimulated by the mechanical stress of the infiltration process. Taken together, these results indicated that reduction of C methylation at these centromeric loci was specifically activated by *P. syringae* pv. *tomato* treatment. They suggested, as well, that the hypomethylation response did not equally affect all 5-mC residues.

We characterized the pattern of *P. syringae* pv. *tomato*-induced hypomethylation within a 350-nucleotide (nt) region of mtDNA harboring sequences from the AFLP clone 3 (Fig. 3B). Bisulfite genomic sequencing was applied to this purpose, and the methylation level of clones obtained from mock- or *P. syringae* pv. *tomato*-treated leaves was compared (Fig. 3C). The selected region contained 51 C residues, including 32 that modified their methylation status upon infection (8 CpG, 6 CpYpG, and 18 CpYpY sites). Among them, 6 sites become hypermethylated (2 CpYpG and 4 CpYpY sites) and 26 hypomethylated (8 CpG, 4 CpYpG, and 14 CpYpY sites). The overall methylation status of the independent clones was 29 to 47% (average 39 ± 8%) for mock-treated samples and 16 to 31% (average 24 ± 5%) for infected tissues. Thus, this genomic region displayed almost 38% reduction of 5-mC content upon infection. Further analysis of changes affecting each methylation context in this region indicated that the 5-mCs located at asymmetric sites contributed

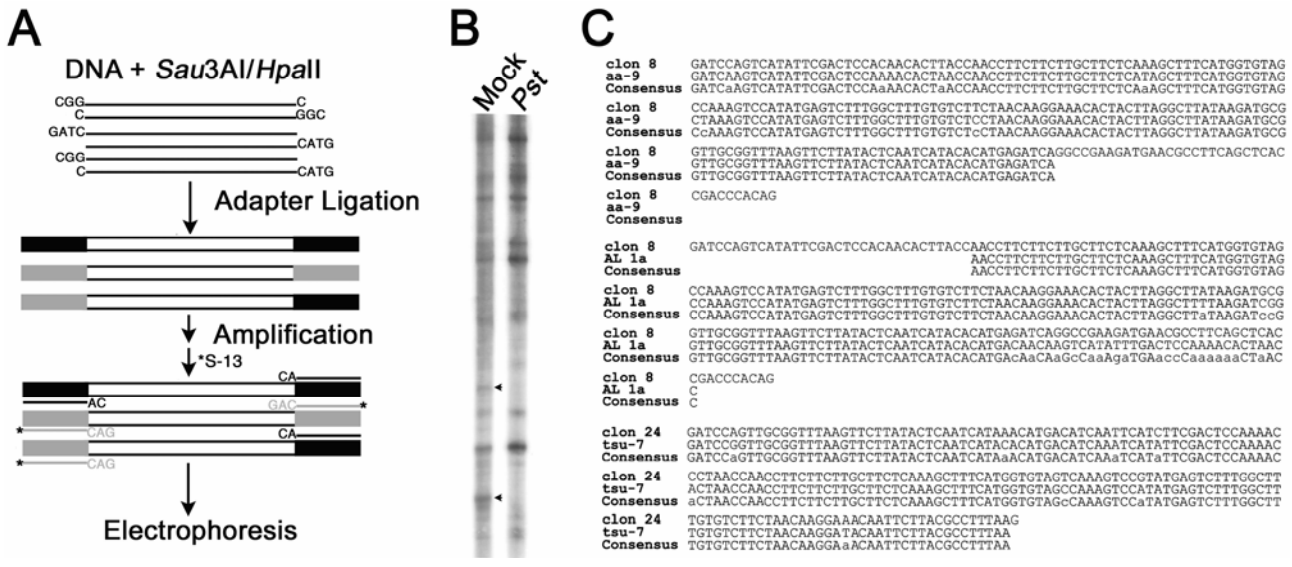

Fig. 2. Plant genomic sequences altering DNA methylation upon infection identified by amplified fragment length polymorphism (AFLP) analysis. **A,** Design of the AFLP strategy applied to monitor the presence of 5-methyl cytosine residues. Digestion products resulting from treatment with *Sau*3AI and *Hpa*II were ligated to *Sau*3AI (gray box) and *Hpa*II (black box) synthetic adapters. Ligation products were amplified by two consecutive rounds of polymerase chain reaction (PCR) with primers complementary to adaptors (H-9: black line; S-13: gray line) which contain two (AC; H-9) or three (CAG; S-13) selectable nucleotides. One radiolabeled primer was included in the second PCR (*S-13 is indicated as example). Products were electrophoresed in sequencing gels and exposed to autoradiography for identification of polymorphic bands. **B,** X-ray image showing a typical AFLP experiment. Mock-inoculated leaves (10 mM $MgCl_2$) (Mock) and *Pseudomonas syringae* pv. *tomato*-treated leaves (10^6 CFU/ml; *Pst*) excised at 24 h postinfiltration were processed in parallel. Arrows show polymorphic bands among these two samples. **C,** Nucleotide sequence of *Arabidopsis thaliana* genomic fragments corresponding to AFLP polymorphic bands 8 and 24 (clones 8 and 24, respectively) containing satellites homologues to the 180-bp repeat such as aa-9 (GenBank AF494843), AL1a (GenBank X04322), and tsu-7 (GenBank AF495273).

to a greater extent to the hypomethylation response (Table 1). In all, 18 asymmetric sites become 50% hypomethylated, whereas 8 CpG and 6 CpYpG symmetric sites became 39 and 36% hypomethylated, respectively.

Changes of the overall plant DNA methylation level induced by *P. syringae* pv. *tomato* treatment.

We evaluated whether *P. syringae* pv. *tomato* infection alters the overall plant genome DNA methylation level. For that pur-

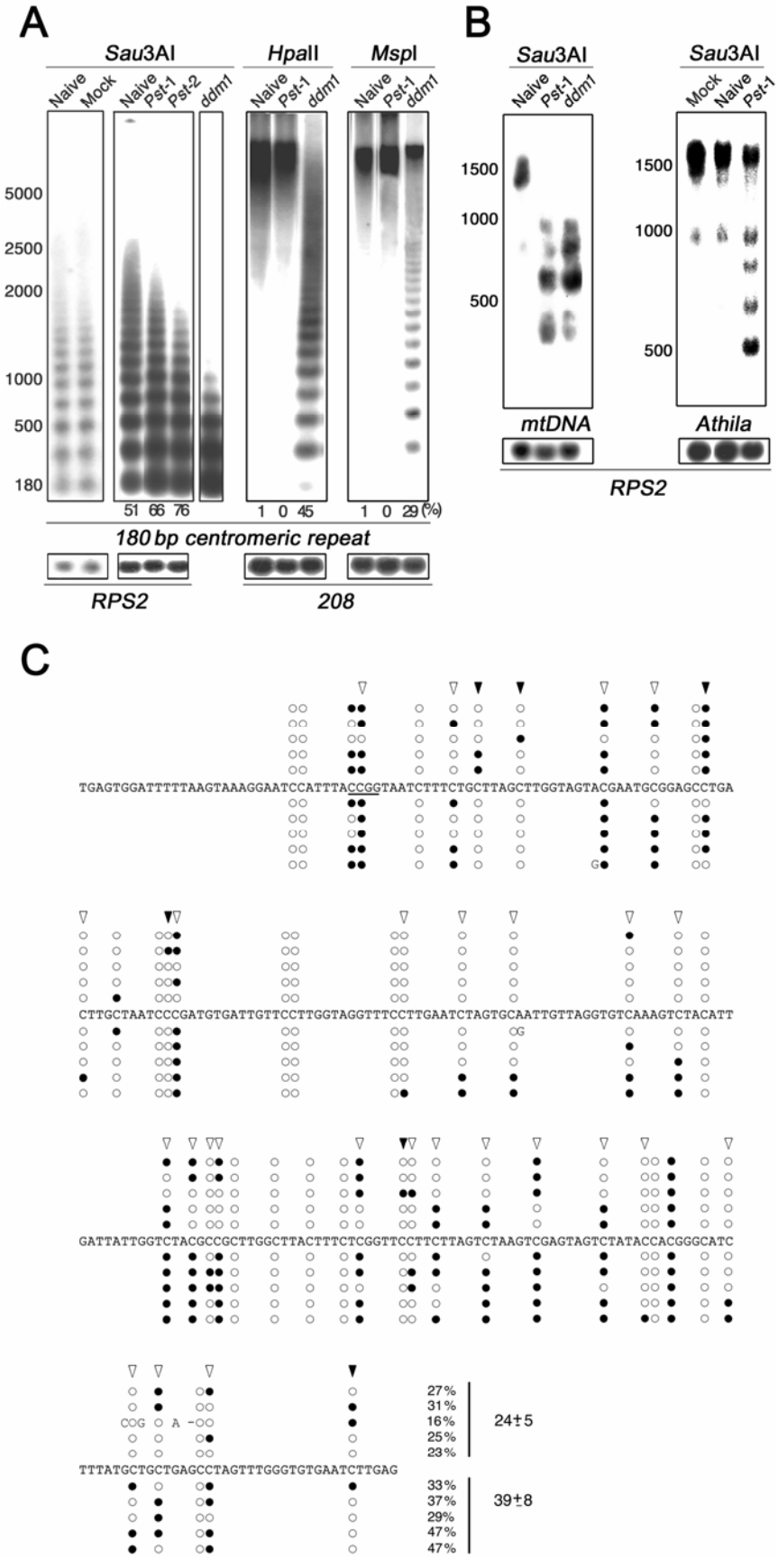

pose, we quantified the 5-mC content in genomic DNA purified from naïve and *P. syringae* pv. *tomato*-treated tissues isolated at 24 hpi by reversed-phase high-performance liquid chromatography (HPLC) assays. Samples belonging to four independent infection experiments were processed and DNA from *ddm1* was included as a control. In accordance with previous reports (Kakutani et al. 1999), we detected 2.37 mol% of 5-mC (with respect to total C content) in the *ddm1* sample and 6.66, 6.28, 6.27, 6.95, or 6.30 mol% (average 6.49 ± 0.30 mol%) in the five naïve wild-type samples. These results indicated that the 5-mC content was almost unaltered by the growth conditions. Interestingly, we observed a consistent reduction of DNA methylation in all four *P. syringae* pv. *tomato*-treated samples analyzed where the 5-mC content was 2.23, 2.45, 4.40, or 4.83 mol%. These values indicated that, at 24 hpi, the 5-mC content is reduced 66, 63, 33, or 26% with respect to the basal levels. Similar hypomethylation values were detected in leaves treated either with different doses of bacteria (10^5 to 5×10^7 CFU/ml; 24 hpi) or exposed to longer infection periods (48 hpi; 10^6 CFU/ml); in none of these cases did the hypomethylation level exceed 66%. Mock-inoculated (10 mM $MgCl_2$) leaves analyzed at 24 hpi were found to contain 6.59 mol% of 5-mC, indicating that hypomethylation was not caused by the mechanical stress generated by the infiltration procedure.

We found that the *P. syringae* pv. *tomato* genome contained undetectable levels of 5-mC. Then, we evaluated whether the 5-mC reduction detected in the plant infected tissues could be caused by dilution of the plant genome with the replicating bacterial genome. We first quantified the *P. syringae* pv. *tomato* content in planta at 24 hpi to further infiltrate the same bacterial content ($[2.6 \pm 0.7] \times 10^6$ CFU/leaf) into naïve leaf tissues (inoculum approximately 10 µl of 2.5×10^8 CFU/ml). Inoculated leaves were excised immediately and processed for 5-mC quantification determining that they contained 6.01 mol% of 5-mC.

In addition, we performed three independent experiments by infiltrating the isogenic avirulent race of *P. syringae* pv. *tomato* carrying the avirulence gene *Rpt2* (*P. syringae* pv. *tomato-avrRpt2*; 10^6 CFU/ml) into Col-0 leaves. In these experiments, a 27, 34, or 67% reduction over the basal 5-mC levels was detected at 24 hpi.

Taken together, these results indicated that the plant genome was the target of 5-mC reduction in infected tissues, and that this change was generated specifically in response to *P. syringae* pv. *tomato* or *P. syringae* pv. *tomato-avrRpt2* treatments.

P. syringae pv. *tomato* treatment induces decondensation of chromocenters.

Because *P. syringae* pv. *tomato* infection disturbed plant centromeric DNA methylation, we tested whether this treatment also modified the organization of centromeric heterochromatin. In *Arabidopsis* interphase nuclei, hypermethylated centromeric and pericentromeric repeats are arranged into heterochromatic and highly compacted chromocenters (CCs). A microscopic inspection of 4′,6-diamidino-2-phenylindole (DAPI)-stained *A. thaliana* mesophyll cells indicated that naïve (Fransz et al. 2002) and mock-inoculated wild-type plants contained an average of 8 CCs per nucleus (Fig. 4A and B). DAPI staining was utilized to characterize cytological features of CCs in *P. syringae* pv. *tomato*-infiltrated tissues at 24 hpi. We observed that nuclei from mesophyll cells presented a marked bias in the distribution of the CC number per nucleus. Whereas nuclei containing ≥7 CCs represented a large majority in naïve and mock-inoculated tissues (88 and 80%, respectively), they constituted a small fraction in *P. syringae* pv. *tomato*-treated tissues (21%) (Fig. 4B). In addition, nuclei with 2 CCs were infrequent in naïve (Fransz et al. 2002) and mock-inoculated tissues, whereas they were the most abundant in infected tissues (Fig. 4B). Typical nuclei from naïve (*i* and *ii*), mock- (*iii*), and bacterial- (*iv* to *ix*) treated samples are shown in Figure 4A. Nuclei from *P. syringae* pv. *tomato*-treated tissues contained either smaller CCs than naïve and mock-treated tissues (*iv* and *vii*) or less than 7 CCs (*v* and *viii*). In addition, we evaluated the effect on plant CC structure caused by infiltration of similar doses (10^6 CFU/ml) of *P. syringae* pv. *tomato-avrRpt2* or the nonpathogenic mutant *P. syringae* pv. *tomato hrpL*$^-$. Reduction of the number of CCs per nuclei was stimu-

Fig. 3. Hypomethylation of centromeric and pericentromeric repeats upon infection with *Pseudomonas syringae* pv. *tomato*. **A** and **B,** Southern blot assays were developed with DNA (3 µg/well in A left panel and 10 µg/well in remaining panels) isolated from wild-type naïve, mock-, or *P. syringae* pv. *tomato*-infiltrated tissues (*Pst*-1, 10^6 CFU/ml; *Pst*-2, 5×10^6 CFU/ml) collected at 24 h postinfection (hpi). A representative sample showing the hypomethylation level of *ddm1* DNA was included. Digestions were performed with *Sau*3AI (A and B), *Hpa*II (A), or *Msp*I (A). For each probe, similar results were observed in three independent experiments. Blots initially were hybridized with probes from the *RPS2* gene or the 208 amplified fragment length polymorphism (AFLP) clone to control equal digestion and loading, stripped, and rehybridized with probes from the AFLP clone 8 (180-bp centromeric repeat), mitochondrial (mt)DNA (AFLP clone 3), or *Athila* (X81801.1). Percent values shown in A refer to the abundance of low molecular bands in each well. **C,** Mapping of 5-methyl cytosine (5-mC) residues in the top strand of a 350-nucleotide mtDNA genomic region (position 67,131 to 67,481 GI: AC007143). Rows represent the status of methylation of individual clones obtained by polymerase chain reaction amplification of bisulfite-treated DNA. Black and white circles represent methylated and unmethylated C residues, respectively. Sequence polymorphisms are indicated for each clone. Clones from *P. syringae* pv. *tomato*-infected (10^6 CFU/ml) or mock-inoculated (10 mM $MgCl_2$) leaves isolated at 24 hpi are shown above and below the consensus sequence, respectively. Black and white triangles indicate sites displaying hyper- or hypomethylation in infected samples, respectively. The *Hpa*II/*Msp*I restriction site (underlined) does not evidence major methylation changes between both treatments. The percentage of 5-mC ([5-mC/5-mC+C] × 100) in each individual clone is shown at the end of each row. The mean values ± standard deviation for each treatment show significant differences at $P < 0.05$ according to Student's *t* test.

Table 1. Cytosine methylation status at mitochondrial DNA in mock- and *Pseudomonas syringae* pv. *tomato*-treated samples

	Number of sites		Methylation range[a]		
Site	**Total[b]**	**Modified[c]**	**Mock**	***P. syringae* pv. *tomato***	**Δ Methylation (%)[d]**
CpG	9	8	38 to 40	23 to 40	–39
CpYpG[e]	7	6	14 to 30	9 to 30	–36
CpYpY[e]	35	18	38 to 90	19 to 90	–50

[a] Fraction of 5-methyl cytosine (5-mCs) to total C residues from all five clones, for the sites described in c.
[b] Total number of sites for each consensus.
[c] Number of sites showing variations in the amount of methylated residues among the five clones from mock- and *P. syringae* pv. *tomato*-treated samples.
[d] Percent differences in the 5-mC content between mock- and *P. syringae* pv. *tomato* -treated samples.
[e] Y: A, T, or C.

lated by *P. syringae* pv. *tomato-avrRpt2* (*vi*). In contrast, this response was not induced by *P. syringae* pv. *tomato hrpL*$^{-}$ (*ix*), even if higher bacterial concentrations were applied into leaf tissues (5×10^8 CFU/ml) (not shown).

To gain sensitivity in the analysis of CC decondensation, we quantified the CC fraction in nuclei from naïve and *P. syringae* pv. *tomato*-infected tissues at 24 hpi using the MetaMorph Imaging software. For individual nuclei, the total area covered by CCs was determined in relation to the area of the entire nucleus. Similar quantitative analysis has been used previously to determine heterochromatin content in *A. thaliana* interphase nuclei (Fransz et al. 2003; Soppe et al. 2002). The CC fraction corresponding to *P. syringae* pv. *tomato*-treated tissues (3.19 ± 0.80) was approximately 60% lower than that determined in naïve tissues (7.97 ± 2.32). Thus, treatment of leaf tissues with *P. syringae* pv. *tomato* suspensions caused major decondensation of centromeric heterochromatin at 24 hpi.

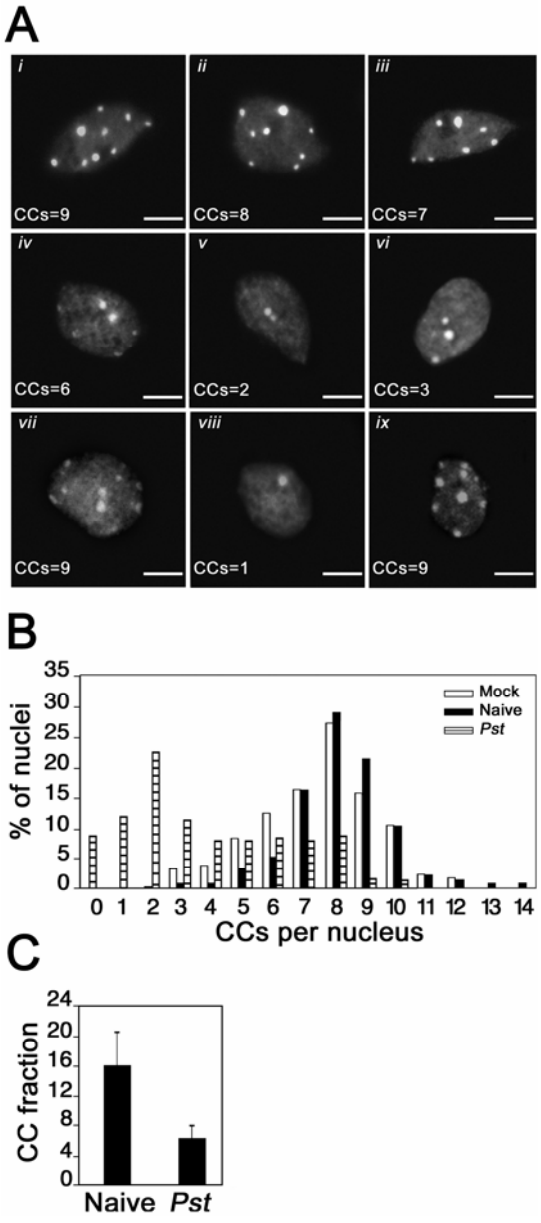

Fig. 4. *Pseudomonas syringae* pv. *tomato* and *P. syringae* pv. *tomato-avrRpt2* (10^6 CFU/ml) induce decondensation of plant chromocenters (CCs). **A,** Staining by 4′,6-diamidino-2-phenylindole of mesophyll nuclei from *Arabidopsis thaliana* wild-type tissues. Samples correspond to naïve (*i* and *ii*), mock- (*iii*), *P. syringae* pv. *tomato*- (*iv* and *v*), *P. syringae* pv. *tomato-avrRpt2*- (*vi*), or *P. syringae* pv. *tomato hrpL*$^{-}$- (*ix*) treated leaves. Samples from 5-bromo-2′-deoxyuridine-fed plants (150 μM; 24 h) further infiltrated with *P. syringae* pv. *tomato* also are included (*vii* and *viii*). **B,** Distribution of the number of chromocenters (CCs) per nuclei in naïve (black bars), mock- (white bars), and *P. syringae* pv. *tomato*- (*Pst*; striped bars) treated leaves at 24 h postinfection. **C,** Heterochromatin content of naïve and *P. syringae* pv. *tomato* (*Pst*)-treated leaves. Values represent the relative percentage of CC areas with respect to the entire nucleus area and indicate medium ± standard deviation. Samples show significant differences at $P < 0.01$ according to Student's *t* test.

Hypomethylation upon infection is not associated with DNA replication.

Reduction of 5-mC induced by treatment with *P. syringae* pv. *tomato* could result from either a process involving DNA replication without maintenance of DNA methylation (passive demethylation) or a mechanism removing methylated residues from the DNA under nonreplicative conditions (active demethylation). To gain insight into this plant response, we evaluated whether hypomethylation observed under infection was accompanied by plant DNA replication. First, we evaluated whether *P. syringae* pv. *tomato*-treated tissues expressed genes considered as markers for DNA replication such as histone H4 (*H4*) and cyclin D3;1 (*CycD3;1*). Activation of *H4* is confined to the S phase of the mitotic cell cycle (Reichheld et al. 1995; Riou-Khamlichi et al. 1999), whereas *CycD3;1* becomes induced specifically in proliferating *Arabidopsis* tissues (Dewitte et al. 2003). When the expression of both genes was analyzed by Northern blot assays in naïve and bacterial challenged tissues isolated at 6, 12, 18, or 24 hpi, none of them was found to be activated (Fig. 5A).

To reach more than 50% of passive demethylation in 24 hpi, the plant genomic content should be duplicated more than once over this period. We formally evaluated whether, in infected tissues, hypomethylation (30 to 66%) takes place in the presence of DNA replication, by quantifying the incorporation of 5-bromo-2′-deoxyuridine (BrdU). Two groups of adult plants were fed with BrdU (discussed below) and leaves of similar developmental stage from each group were either mock- or pathogen-inoculated. Inoculated leaves were excised 24 h later and were processed by indirect immunofluorescence with anti-BrdU antibodies to determine incorporation of BrdU into newly synthesized DNA strands. These samples contained less than 1% of cells incorporating BrdU without significant differences among both values (mock: $8.82 \pm 2.41 \times 10^{-1}$, n = 900; *P. syringae* pv. *tomato*: $9.53 \pm 2.71 \times 10^{-1}$, n = 782) (Fig. 5B). These *P. syringae* pv. *tomato*-infected samples evidenced DNA hypomethylation according to Southern blot assays (*Sau*3AI; 180-bp repeat) as well as chromocenter decondensation (Fig. 4A, vii and viii). These features indicated that BrdU did not abolish the plant genomic alterations induced by the pathogen. However, BrdU (150 μM) could have deleterious effects on *P. syringae* pv. *tomato* virulence. We analyzed this possibility by comparing disease-associated cell death patterns (Fig. 1, 24 and 96 hpi) and bacterial growth in planta (Fig. 5C, 96 hpi) in plants treated or not with BrdU. Identical responses were detected in both groups of plants, indicating that major *P. syringae* pv. *tomato* virulence functions were not attenuated by BrdU treatment.

This group of results indicated that the DNA hypomethylation response detected in *A. thaliana* tissues treated with *P. syringae* pv. *tomato* involved an active demethylation process.

DISCUSSION

Using AFLP assays, methylation sensitive restriction enzymes, bisulfite genomic sequencing, and HPLC assays, we demonstrated here that *A. thaliana* leaf tissues display DNA

hypomethylation upon attack by *P. syringae* pv. *tomato*. Reduction in 5-mC from the genome of infected plants has been described at the biochemical level for wilt infection in cotton (Guseinov and Vanyushin 1975). Here, we provide a complete characterization of bacterial-induced plant hypomethylation by describing molecular, biochemical, and cytological features associated with this response at 24 hpi.

We characterized three repetitive centromeric sequences that become demethylated in response to *P. syringae* pv. *tomato*. These are the 180-bp repeat, mtDNA, and *Athila* retrotransposon sequences, which concentrate methylated DNA in the *A. thaliana* genome (Bender 2004). Patterns of *Sau*3AI cleavage inhibition indicated that all these sequences lost 5-mC residues placed on 5′-GATC-3′ sites. At the molecular level, *P. syringae* pv. *tomato*-induced hypomethylation showed similarities and differences with hypomethylation of *ddm1* (impaired in a SWI/SNK-like chromatin remodeling protein). Although demethylation at *Sau*3AI sites of mtDNA sequences was similar in both cases, pathogen-treated samples had lower demethylation at *Sau*3AI sites and no demethylation of *Hpa*II or *Msp*I sites of the 180-bp repeats compared with *ddm1* samples. These results pointed out the existence of differences in the molecular targets of *P. syringae* pv. *tomato*- and *ddm1*-induced hypomethylation. Accordingly, variations in the molecular contexts of hypomethylation responses were described for different *Arabidopsis* hypomethylated genotypes (Bender et al. 2004).

Results from Southern blot assays suggested that the *Sau*3AI sites analyzed in these experiments (Fig. 3A and B) might not constitute the main targets of *P. syringae* pv. *tomato*-induced demethylation, and that demethylation also might affect other sites. These results also indicated that demethylation might not equally affect all the 5-mC contexts. In agreement with this observation, using bisulfite genomic sequencing, we determined that, within a 350-nt fragment of the mtDNA, the 5m-C residues more affected by demethylation were those located at asymmetric sites (Table 1). Methylated Cs located in asymmetric consensus might be the most abundant in the *Arabidopsis* genome (Luo and Preuss 2003) and their demethylation at repetitive sequences might contribute importantly to the genomic response detected by HPLC in the infected tissues. In agreement with these observations, hypomethylation of cotton genomic sequences in *Verticillium* spp.-infected tissues was proposed to involve nonrandom distributed 5-mCs (Guseinov and Vanyushin 1975).

The 180-bp unit, *Athila*, and mtDNA are sequences containing near 20,000, 500, and 3 copies, respectively, in the *Arabidopsis* genome (Hall et al. 2003; Martinez-Zapater et al. 1986; Stupar et al. 2001; The Arabidopsis Genome Initiative 2000). The first two repeats are found in all five centromeres, whereas the mtDNA (620 kb) is present at the pericentric region of chromosome 2. The mtDNA fragment here analyzed is contained in the BAC T17H1, which might be represented at least three times in the genome (Stupar et al. 2001). Thus, high, medium, and low repetitive sequences nested in centromeric and pericentromeric heterochromatin (Bender 2004) were found to display *P. syringae* pv. *tomato*-induced hypomethylation. Whether sequence nature (repetitive), chromatin structure (heterochromatin), or both features provide particular cues for defining the plant genomic targets of this response deserves further analysis. Considering that AFLP experiments also revealed nonrepetitive, noncentromeric sequences altering methylation under infection, it is expected that such changes are not exclusive to centromeric DNA. Interestingly, along the characterization of methylation patterns of mtDNA sequences, we found that Cs located at 5′-GATC-3′ sites were demethylated in the *ddm1* background. This result is consistent with the fact that the DDM1 chromatin remodeling factor maintains methylation of CpG and non-CpG contexts in both single-copy genes and repetitive units, including centromeric repeats (Bender 2004; Vongs et al. 1993).

The mechanisms leading to plant DNA hypomethylation upon infection as well as the consequences of this response are at present unknown. We found unlikely the reduction of 5-mC results from specific degradation of the methylated residues because DNA degradation never was observed by Southern blots in *P. syringae* pv. *tomato*-treated samples. In a similar sense, DNA hypomethylation does not appear to be a consequence of *P. syringae* pv. *tomato*-induced necrosis because it takes place early during infection (24 hpi). At this time, the large majority of cells from the infected tissues remain alive and massive plant cell death takes place several hours later (96 hpi). We analyzed whether tissues activating hypomethylation displayed DNA replication; if this was true, 5-mC reduction could result from a passive demethylation process (absence of de novo DNA methylation). This was found a priori unlikely based on two main considerations. First, reduction of 5-mC content in infected tissues did not equally affect all methylated residues (Fig. 3A and C). Second, two replication cycles might occur in 24 h in expanded leaf tissues infected with *P. syringae* pv. *tomato* to reach 66% of hypomethylation. However, during *Arabidopsis* leaf development, nearly 88% of cells divide only once in 24 h (Autran et al. 2002). We performed experiments to demonstrate the absence of DNA replication in *P. syringae*

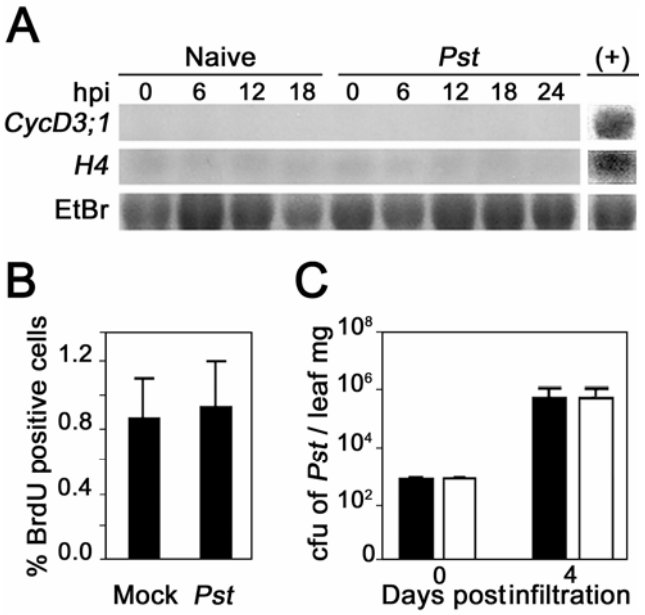

Fig. 5. Adult *Arabidopsis thaliana* leaf tissues treated with *Pseudomonas syringae* pv. *tomato* (10^6 CFU/ml) do not display features of DNA replication at 24 h postinfection (hpi). **A,** Northern blot assays analyzing the accumulation of *CycD3;1* and *H4* transcripts in naïve and *P. syringae* pv. *tomato* (*Pst*)-infiltrated tissues. Samples were excised at the indicated hours after pathogen infiltration. Naïve samples were monitored at different time points to control the eventual circadian expression of these genes. RNA isolated from whole root tissues was used as a positive control (+). Loading was monitored by gel ethidium bromide staining. **B,** Plants were fed with 5-bromo-2′-deoxyuridine (BrdU) (150 μM; 24 h) and further infiltrated with vehicle (mock) or *P. syringae* pv. *tomato* (*Pst*) suspension. Infiltrated tissues collected at 24 hpi were utilized to determine BrdU incorporation by indirect immunofluorescence. The proportions of nuclei incorporating BrdU were compared. Data represent the mean ± standard deviation (SD) of four independent experiments. **C,** Growth of *P. syringae* pv. *tomato* (*Pst*) in leaf tissues of untreated plants (black bars) or plants treated with 150 μM BrdU (white bars) at 4 days after pathogen inoculation. Data represent the mean ± SD of three independent experiments.

pv. *tomato*-treated tissues. Molecular markers of DNA replication, such as accumulation of histone *H4* and cyclin *CycD3;1* transcripts, were not detected in *P. syringae* pv. *tomato*-treated hypomethylated tissues (Fig. 5A). These markers also became induced during endoreduplication, an alternative form of cell cycle generating endopolyploid cells when DNA replication occurs without the intervention of mitosis. The absence of *H4* and *CycD3;1* expression in infected tissues argued against the activation of either a classical mitotic cell cycle or the shorter circuit of endoreduplication. Accordingly, DNA replication was not detected by quantification of BrdU in *P. syringae* pv. *tomato*-treated tissues (Fig. 5B). Then, because DNA hypomethylation is achieved without significant DNA synthesis, it may be generated by an active demethylation process affecting a significant population of cells from the infected tissues. Several reports support the existence of active demethylation in plants (Cui and Fedoroff 2002; Gong et al. 2002; Zluvova et al. 2001). However, the biochemical nature of such demethylating activity is controversial. A good candidate for such function in *A. thaliana* is the 5-mC DNA glycosylase, proposed to mediate particular demethylation events by excision of 5-mC residues from the DNA molecule (Gong et al. 2002). Our results point out the *Arabidopsis–Pseudomonas* pathosystem as a useful model to characterize the components leading to active DNA demethylation in plants.

It is plausible that conditions promoting DNA hypomethylation affect basic plant genomic functions such as avoidance of recombination between repetitive units, gene expression, generation of new epialleles, or others (Bender 2004). DNA methylation maintains recombination-deficient heterochromatin structures (Bender 2004). Then, it is likely that *P. syringae* pv. *tomato*-induced heterochromatin decondensation (Fig. 4) promotes increased DNA recombination at centromeric regions harboring an important level of resistance genes. This structural alteration might involve hypomethylation of peri/centromeric sequences as it was reported to occur in *Arabidopsis ddm1* and *met1* (deficient in a maintenance DNA methyltransferase) mutants (Fransz et al. 2003; Soppe et al. 2002). In a similar sense, exacerbated DNA rearrangements occurring under stress conditions might enhance genome plasticity and genetic variability in the progeny of stressed organisms (Grandbastien et al. 1997; Kovalchuk et al. 2003; Lucht et al. 2002; Yoder et al. 1997). *Arabidopsis* leaf tissues exposed to the oomycete *Peronospora parasitica* or to chemical inducers of biotic defenses enhance somatic recombination (Lucht et al. 2002), and similar responses were found in tobacco plants supporting viral infections (Kovalchuk et al. 2003).

Enhanced expression of retrotransposons occurs in tobacco, *Arabidopsis*, and tomato cells exposed to pathogen attack (Grandbastien et al. 1997). Similarly, hypomethylated *Arabidopsis* mutants activate normally methylated and silent transposons concentrated at peri/centromeric heterochromatic domains, including the retrotransposon *Athila* (Bender 2004). Although we found that *Athila* becomes demethylated upon *Pseudomonas syringae* pv. *tomato* infection (Fig. 3B), we did not detect *Athila* expression in infected tissues. Similarly, we did not find altered transcription of any of the 11 peri/centromeric single-copy genes located inside the genetic centromeres embedded in highly methylated genomic domains. The genes analyzed in these assays were At2g07750 and At2g07690 (BAC T12J2); At2g07560 (BAC F9A16); At3g42170 (BAC T27B3), At4g05120, At4g05160, and At4g05180 (BAC C17L7); At4g04910 (BAC T1J1); At5g32440 and At5g32450 (BAC F18O9); and At5g30510 (BAC F19I11) (The Arabidopsis Genome Initiative 2000). Thus, although we cannot rule out the possibility that some of these loci become induced in a minor population of infected cells, or in a transient manner, they do not exhibit net transcriptional changes under the hypomethylation condition analyzed here. In a similar sense, we cannot discard the idea that these major chromatin changes could alter the expression level of genes located at other genomic domains.

As mentioned above, genome hypomethylation might result in the generation of new epigenetic information. Methylation defects can be perpetuated stably through mitosis and meiosis in *A. thaliana* (Kakutani et al. 1996, 1999; Richards 1997), contributing to the generation of advantageous epialleles. Consistent with this hypothesis, a vast diversification of gametes is generated in demethylated plants carrying a null mutation for the MET-1 gene (*met-1*) (Saze et al. 2003), and overexpression of a disease resistance-like gene associated with activation of defenses occurred in the heritable epigenetic variant *bal*, generated in an inbred population of *ddm1* plants (Stokes et al. 2002). Therefore, novel epigenetic information could be produced in aerial *P. syringae* pv. *tomato*-infected tissues and, in case this change affects germ cell precursors able to survive the infective process, this new information could be sexually transmitted to the progeny.

Plant DNA demethylation and reduction in CC number were activated in a similar manner by either virulent or avirulent races of *P. syringae* pv. *tomato*, indicating that they might not constitute *R*-gene-mediated defenses. Moreover, reduction in CC number was not stimulated by the single perception of bacteria in the apoplast, but required HrpL-dependent functions. HrpL encodes an alternative RNA polymerase sigma factor that regulates the expression of many virulent genes of *P. syringae* pv. *tomato* DC3000, including the components of the type III secretion system allowing translocation of bacterial effectors into the host cells (Alfano and Collmer 2004). Our results suggest that either structural or functional roles depending on HrpL, such as those previously described, might be involved in the stimulation of host chromatin alterations. However, whether these responses contribute to enhance host defenses or are produced as a consequence of *P. syringae* pv. *tomato* pathogenic functions remains to be established.

MATERIALS AND METHODS

Plant material, bacterial manipulation, and cell death.

A. thaliana plants were grown in soil under cycles of 9 h of light and 15 h of dark at 23ºC for 6 to 8 weeks in incubators conserved with strict hygiene. The virulent *P. syringae* pv. *tomato* DC3000 strain and its isogenic avirulent race carrying the avirulent gene *Rps2* (*P. syringae* pv. *tomato-avrRpt2*), as well as the *P. syringae* pv. *tomato hrpL*$^-$ mutant (KP411 *hrpL*$^-$ strain obtained from S.-Y. He, Michigan State University, East Lansing, MI, U.S.A.), were used in these studies. Bacterial cultures were grown overnight in King's B medium with tetracycline at 10 μg/ml and rifampicin at 100 μg/ml, washed twice in 10 mM $MgCl_2$, and resuspended to the final concentration in the same solution. Bacterial suspensions were infiltrated at the abaxial surface of leaves using a 1-ml needleless syringe. Unless otherwise indicated, whole leaves were infiltrated with bacteria at 10^6 CFU/ml and 10 mM $MgCl_2$. Mock inoculations were performed by using 10 mM $MgCl_2$. Bacterial growth curves and trypan blue staining used to monitor cell death were developed as described previously (Alvarez et al. 1998). For each HPLC determination, approximately 100 naïve or infiltrated leaves (*P. syringae* pv. *tomato* at 10^6 CFU/ml) were processed. To determine bacterial content in planta in each group of infected plants, 15 infiltrated leaves were excised at 24 hpi, macerated, and processed in three independent groups (5 leaves each) to extract and quantify bacteria (Alvarez et al. 1998). A mean value then was obtained for each group of infected plants, and three independ-

ent infection experiments were processed to obtain the media ± standard deviation of these values ($2.6 \pm 0.7 \times 10^6$).

AFLP analysis.

The AFLP protocol included basic steps described previously (Cervera et al. 2002) with some modifications. DNA (100 ng) treated with *Sau*3AI and *Hpa*II (8 U of each, 16 h at 37ºC) was ligated with adapters (13.3 µM *Hpa*II or *Sau*3AI adapters, 3 U of T4DNA ligase, 1 mM ATP, 30 mM Tris-HCl, pH 7,8, 10 mM $MgCl_2$, and 10 mM dithiothreitol [DTT]; 16 h at 23ºC; 40 µl of reaction). Adapters were prepared by incubating equimolar amounts of complementary oligonucleotides. That is, 5′-CGC TCAGGACTCAT-3′ and 5′-GACGATGAGTCCTGAG-3′ oligonucleotides for the *Hpa*II adaptor, and 5′-GATCCTCAGGACT CAT-3′ and 5′-GACGATGAGTCCTGAG-3′ for the *Sau*3AI adaptor. Adapted DNA was used in two consecutive PCR reactions, including the H-9 (5′-GATGAGTCCTGAGCGGAC-3′) and S-13 (5′-GATGAGTCCTGAGGATCCAG-3′) primers, containing two and three selectable nucleotides, respectively. One radiolabeled primer (Hpa9 or Sau13) was used in the second PCR reaction (60 µl of labeling reaction containing 300 ng of oligonucleotide, 200 µCi γ ^{32}P-ATP, 40 U of T4 polynucleotide kinase, 70 mM Tris-HCl, pH 7.6, 10 mM $MgCl_2$, and 5 mM DTT; 1 h at 37°C). The first PCR reaction (20 µl) contained 2.5 ng of adapted DNA, 30 ng of Hpa9 and Sau13 primers, 0.5 U of Taq DNA polymerase, 20 mM Tris-HCl, pH 8.4, 50 mM KCl, 2,5 mM $MgCl_2$, and 500 µM dNTPs. The second PCR was performed under the same conditions using 0.5 µl of the first reaction as template. Amplification was performed in both cases by 36 cycles of: 30 s at 94ºC, 30 s at annealing temperature (first cycle, 65ºC; 11 cycles with a 0.7ºC reduction/cycle; and 24 cycles at 56ºC), and 1 min at 72ºC. Amplified products (5 µl of reaction) were loaded on a 6% denaturing polyacrylamide sequencing gels. Two sequential loading steps were applied to resolve approximately 100 bands per assay. Highly reproducible pattern of bands were obtained under these conditions for a wide range of DNA content (10^2 to 4×10^4 *A. thaliana* genomic equivalents). Thirteen polymorphic bands (2, 3, 4, 8, 9, 10, 11, 12, 14, 19, 20, 24, and 25), consistently observed in at least two independent experiments, were excised from gels. Bands 2, 3, 4, 11, 12, and 23 were excised from samples of *P. syringae* pv. *tomato*-treated tissues isolated at 24 hpi, whereas bands 8, 9, 10, 20, and 24 were from samples corresponding to naïve tissues. DNA was eluted from these bands and reamplified with H9 and S13 primers. An aliquot of these PCR products was radiolabeled and used as probes in Southern blots containing *Mbo*I-digested DNA from *A. thaliana* and *P. syringae* pv. *tomato*. Because probes from bands 2, 4, 11, and 12 detected the *P. syringae* pv. *tomato* genome, these bands were discarded. DNAs contained in the remaining nine bands were cloned and sequenced (more than three clones per band). In addition, four bands (14, 18, 19, and 25) also were discarded because their corresponding subclones either contained artifactual products of ligation (noncontiguous genomic fragments separated by 5′-GATC-3′ or 5′-CCGG-3′ sites) or different sequences. Thus, DNAs contained in bands 3, 8, 9, 10, 20, 23, and 24 were considered to be possible targets of altered methylation in the *A. thaliana* genome.

Nucleic acids and Southern and Northern blots.

A. thaliana and *P. syringae* pv. *tomato* genomic DNA were purified by phenolic extraction methods (Dellaporta et al. 1983). Total RNA was isolated as described previously (Alvarez et al. 1998). Southern and Northern blots contained 10 µg of DNA and 40 µg of total RNA, respectively, per well. Probes corresponded to PCR products of *Athila* (accession X 81801.1) (Tompa et al. 2002) (5′-ttcttctccaactccagg-3′ and 5′-TACCCT TTGTTGGAGCCG-3′ primers) and RPS2 (5′-GAGCGAGAA ATCATCG-3′ and GTCTATCTCTTCCCAG-3′) genes as well as fragments of *H4* and *CycD3;1* genes (Riou-Khamlichi et al. 1999). X-ray films from Southern blots hybridized with the 180-bp probe were scanned to quantify the signal intensity along each well (Scion Image, Scion Corp. Frederick, MD, U.S.A.). The percentage values of low molecular weight bands (<1 kb for *Sau*3AI and <2.0 kb for *Hpa*II and *Msp*I) with respect to total signal intensity in each well were determined.

Bisulfite genomic sequencing.

DNA was purified from *P. syringae* pv. *tomato*- or mock-inoculated leaves (24 hpi) and treated as described by Luo and Preuss (2004) with minor modifications. Briefly, DNA was digested with *Eco*RI, denatured (0.1 M NaOH; 15 min at 20ºC), and treated with bisulfite (1.2 ml of 4 M $NaHSO_3$, 500 µM hydroquinone, pH 5.0; 12 h at 50ºC). DNA was purified using the Wizzard DNAClean-up kit (Promega Corp., Madison, WI, U.S.A.), incubated in 0.3 M NaOH (20ºC for 10 min), neutralized with ammonium acetate (750 mM, pH 7.5), precipitated with ethanol, and resuspended in milliQ H_2O (100 µl). An aliquot of this sample (5 µl) was used for strand-specific PCR amplification. PCR fragments amplified from three independent infection experiments were cloned (TOPO kit, Invitrogen, Carlsbad, CA, U.S.A.) and sequenced. PCR conditions and primer sequences are available upon request.

Determination of 5-mC content by HPLC.

Two groups of plants grown under identical conditions were either infiltrated with *P. syringae* pv. *tomato* (discussed above) or maintained without any treatment (naïve) to be further processed in parallel in HPLC experiments. *A. thaliana* and *P. syringae* pv. *tomato* genomic DNA were purified (Dellaporta et al. 1983) and dialyzed against Tris-EDTA buffer (2 × 30,000 vol.). Nucleoside-enriched fractions were obtained by enzymatic hydrolysis of DNA according to the 4-h two-enzyme method described by Gehrke and associates (1984) with minor modifications. Briefly, DNA (40 µg in water) was boiled for 2 min and immediately incubated in ice. Samples were treated with 2 U of Nuclease P1 (Sigma-Aldrich, St. Louis) for 2 h at 37ºC in a medium containing 18 mM sodium acetate (pH 5.3) and 1 mM zinc sulfate. After adjusting pH to 8.3 with 0.5 M Tris-HCl, 10 U of calf intestinal alkaline phosphatase (Promega Corp.) was added and samples maintained for 2 h at 37ºC. Proteins were removed by precipitation with 8 volumes of 96% ethanol and further centrifugation at 12,000 rpm for 10 min. Samples were dried in Speed Vac and either stored at –20ºC or resuspended in 18 µl of water for immediate analysis. These nucleoside-enriched samples were analyzed by HPLC using a C-18 Ultrasphere-ODS-Pharmacia, Altex (4.6 by 250 mm) column. A 20-min isocratic gradient of buffer A (2.5% methanol, 50 mM KH_2PO_4, pH 3.7) followed by 20 min of linear gradient of buffer B (8% methanol, 50 mM KH_2PO_4, pH 3.7), and a subsequent 20-min isocratic gradient of buffer B was applied. Commercial dA, dT, dC, dG, and 5-mC (Sigma-Aldrich) were used as standards. Values were calculated by integration of peak areas of absorbance at 280 nm using the Peak Simple program. Percentages of 5-mC content (5-mC/5-mC+dC) were normalized for absorbance differences between dC and 5-mC. For each sample, the informed value represents the average of two independent determinations. When the 5-mC levels were referred to the dT content, similar percentages of reduction were detected. Percentage of 5-mC reduction in the *P. syringae* pv. *tomato*-treated samples was estimated with respect to the corresponding naïve samples.

Cytochemistry and immunocytochemistry.

Leaves at similar developmental stages were used for DAPI staining and immunocytochemical experiments. For DAPI

staining, leaves were excised and fixed in ethanol/acetic acid (3:1) for 24 h at 4ºC and further stored at –20ºC. Leaves were washed in distilled water (three times, 10 min each) and 0.01 M citrate buffer, pH 5 (three times, 15 min each), and treated with enzymes (1.5% Macerozyme R-10, 1.5% Cellulase Onozuka RS; Yakult Pharmaceutical, Tokyo) in 0.01 M buffer for 15 to 20 min at 37ºC. All DAPI-bright spots found at all the different optical sections of a nucleus having a size similar to that of the CCs found in nuclei of naïve tissues were quantified.

DNA replication was evaluated by incorporation of BrdU. Whole 4- to 5-week-old plants grown in soil were incubated for 4 or 24 h in 3 ml of 150 µM BrdU (in water) before washing roots with water as described by Nagar and associates (2002). Similar results were obtained for both BrdU incubation periods. After renewing the BrdU solution, plants were treated with either *P. syringae* pv. *tomato* (10^6 CFU/ml) or $MgCl_2$ (mock) to be maintained for an additional 24 h. At this time, infiltrated leaves were excised, fixed in 4% paraformaldehyde for 24 h at 4ºC, washed (0.01 M citrate buffer, pH 5.6, 10 min) and softened in enzyme solution (1.5% cellulase/1.5% mazerozyme, 37ºC, 15 min). Digested leaf material was spread on slides as described by Moscone and associates (1996). The following steps were performed at 37ºC. Slides were treated with 3% paraformaldehyde (30 min), washed with 1× phosphate-buffered saline (PBS), pH 7.2 (three times, 5 min each), permeabilized (0.25% triton X100 in 1× PBS, 10 min), washed (1× PBS, three times, 5 min each), blocked (5% bovine serum albumin in 1× PBS for 2 h), and washed (1× PBS, three times, 5 min each). Cellular DNA was denatured (0.5% triton X100, 2 N HCl, 15 min) and slides were washed (1× PBS, 10 times, 2 min each). To detect incorporation of BrdU, a primary mouse anti-BrdU antibody (Roche Biochemicals, Mumbai, India; 1/400) and Alexa 488 goat anti-mouse conjugate (Molecular Probes, Eugene, OR, U.S.A., 1/250) were used. Slides were mounted in mounting fluid (Light Diagnostics, Salt Lake City, UT, U.S.A.) supplemented with DAPI (1 µg/ml).

Digital images in grayscale were analyzed with MetaMorph Imaging software (Universal Imaging, Downingtown, PA, U.S.A.) adapted to measure the number of CCs per nuclei and area of nuclei and CCs. The cut-off value of a minimal stained area considered as a CC was determined manually by analyzing the average of the area of CCs from 100 wild-type nuclei. This value was introduced in the filter range area window of the program and the number and area of CCs from 50 nuclei isolated from untreated and *P. syringae* pv. *tomato*-infected (10^6 CFU/ml) leaves was determined automatically. The total nuclei area occupied by CCs was determined in each nucleus by adding CC areas and dividing the result in the whole nuclei area. The average of the obtained values from untreated and *P. syringae* pv. *tomato*-infected leaves was reported as the CC fraction.

ACKNOWLEDGMENTS

M. E. Alvarez and A. L. Rosa are senior career investigators of Consejo Nacional de Investigaciones Científicas y Técnicas (CONICET). This work was supported by grants from ANPCyT (PICT 01-10123), Fundación Antorchas, CONICET, and SECyT-UNC. We thank the ABRC for *A. thaliana* Col-0 seed, E. Richards (Washington University, St. Louis, MO, U.S.A.) for *ddm1* seed, J. A. H. Murray (Institute of Biotechnology, University of Cambridge, UK) for *H4* and *CycD3;1* probes, S.-Y. He (Michigan State University) for *P. syringae* pv. *tomato hrpL*⁻ mutant, and J. L. Barra and A. Goldraij for critical reading of the manuscript.

LITERATURE CITED

Alfano, J. R., and Collmer, A. 2004. Type III secretion system effector proteins: Double agents in bacterial disease and plant defense. Annu. Rev. Phytopathol. 42:385-414.

Alvarez, M. E., Pennell, R. I., Meijer, P. J., Ishikawa, A., Dixon, R. A., and Lamb, C. 1998. Reactive oxygen intermediates mediate a systemic signal network in the establishment of plant immunity. Cell 92:773-784.

Autran, D., Jonak, C., Belcram, K., Beemster, G. T., Kronenberger, J., Grandjean, O., Inze, D., and Traas, J. 2002. Cell numbers and leaf development in *Arabidopsis*: A functional analysis of the STRUWWELPETER gene. EMBO (Eur. Mol. Biol. Organ.) J. 21:6036-6049.

Bender, J. 2004. DNA Methylation and epigenetics. Annu. Rev. Plant Biol. 55:41-68.

Bhattacharya, S. K., Ramchandani, S., Cervoni, N., and Szyf, M. 1999. A mammalian protein with specific demethylase activity for mCpG DNA. Nature 397:579-583.

Bird, A. 2002. DNA methylation patterns and epigenetic memory. Genes Dev. 16:6-21.

Brosch, G., Ransom, R., Lechner, T., Walton, J. D., and Loidl, P. 1995. Inhibition of maize histone deacetylases by HC toxin, the host-selective toxin of Cochliobolus carbonum. Plant Cell 7:1941-1950.

Burn, J. E., Bagnall, D. J., Metzger, J. D., Dennis, E. S., and Peacock, W. J. 1993. DNA methylation, vernalization, and the initiation of flowering. Proc. Natl. Acad. Sci. U.S.A. 90:287-291.

Cao, X., and Jacobsen, S. E. 2002. Role of the *Arabidopsis* DRM methyltransferases in de novo DNA methylation and gene silencing. Curr. Biol. 12:1138-1144.

Cervera, M. T., Ruiz-Garcia, L., and Martinez-Zapater, J. M. 2002. Analysis of DNA methylation in *Arabidopsis thaliana* based on methylation-sensitive AFLP markers. Mol. Genet. Genomics 268:543-552.

Cui, H., and Fedoroff, N. V. 2002. Inducible DNA demethylation mediated by the maize Suppressor-mutator transposon-encoded TnpA protein. Plant Cell 14:2883-2899.

Dellaporta, S. L., Wood, J., and Hicks, J. 1983. A plant DNA minipreparation: Version II. Plant Mol. Biol. Rep. 1:19-21.

Dewitte, W., Riou-Khamlichi, C., Scofield, S., Healy, J. M., Jacqmard, A., Kilby, N. J., and Murray, J. A. 2003. Altered cell cycle distribution, hyperplasia, and inhibited differentiation in *Arabidopsis* caused by the D-type cyclin CYCD3. Plant Cell 15:79-92.

Finnegan, E. J., Peacock, W. J., and Dennis, E. S. 1996. Reduced DNA methylation in *Arabidopsis thaliana* results in abnormal plant development. Proc. Natl. Acad. Sci. U.S.A. 93:8449-8454.

Finnegan, E. J., Genger, R. K., Kovac, K., Peacock, W. J., and Dennis, E. S. 1998. DNA methylation and the promotion of flowering by vernalization. Proc. Natl. Acad. Sci. U.S.A. 95:5824-5829.

Fransz, P., De Jong, J. H., Lysak, M., Castiglione, M. R., and Schubert, I. 2002. Interphase chromosomes in *Arabidopsis* are organized as well defined chromocenters from which euchromatin loops emanate. Proc. Natl. Acad. Sci. U.S.A. 99:14584-14589.

Fransz, P., Soppe, W., and Schubert, I. 2003. Heterochromatin in interphase nuclei of *Arabidopsis thaliana*. Chromosome Res. 11:227-240.

Gehrke, C. W., McCune, R. A., Gama-Sosa, M. A., Ehrlich, M., and Kuo, K. C. 1984. Quantitative reversed-phase high-performance liquid chromatography of major and modified nucleosides in DNA. J. Chromatogr. 301:199-219.

Gong, Z., Morales-Ruiz, T., Ariza, R. R., Roldan-Arjona, T., David, L., and Zhu, J. K. 2002. ROS1, a repressor of transcriptional gene silencing in *Arabidopsis*, encodes a DNA glycosylase/lyase. Cell 111:803-814.

Grandbastien, M. A., Lucas, H., Morel, J. B., Mhiri, C., Vernhettes, S., and Casacuberta, J. M. 1997. The expression of the tobacco Tnt1 retrotransposon is linked to plant defense responses. Genetica 100:241-252.

Guseinov, V. A., and Vanyushin, B. F. 1975. Content and localisation of 5-methylcytosine in DNA of healthy and wilt-infected cotton plants. Biochim. Biophys. Acta 395:229-238.

Hall, S. E., Kettler, G., and Preuss, D. 2003. Centromere satellites from *Arabidopsis* populations: Maintenance of conserved and variable domains. Genome Res. 13:195-205.

Johal, G. S., and Briggs, S. P. 1992. Reductase activity encoded by the HM1 disease resistance gene in maize. Science 258:985-987.

Kakutani, T., Jeddeloh, J. A., Flowers, S. K., Munakata, K., and Richards, E. J. 1996. Developmental abnormalities and epimutations associated with DNA hypomethylation mutations. Proc. Natl. Acad. Sci. U.S.A. 93:12406-12411.

Kakutani, T., Munakata, K., Richards, E. J., and Hirochika, H. 1999. Meiotically and mitotically stable inheritance of DNA hypomethylation induced by ddm1 mutation of *Arabidopsis thaliana*. Genetics 151:831-838.

Kovalchuk, I., Kovalchuk, O., Kalck, V., Boyko, V., Filkowski, J., Heinlein, M., and Hohn, B. 2003. Pathogen-induced systemic plant signal triggers DNA rearrangements. Nature 423:760-762.

Lucht, J. M., Mauch-Mani, B., Steiner, H. Y., Metraux, J. P., Ryals, J., and Hohn, B. 2002. Pathogen stress increases somatic recombination frequency in *Arabidopsis*. Nat. Genet. 30:311-314.

Luo, S., and Preuss, D. 2003. Strand-biased DNA methylation associated with centromeric regions in *Arabidopsis*. Proc. Natl. Acad. Sci. U.S.A. 100:11133-11138.
Martienssen, R. A., and Colot, V. 2001. DNA methylation and epigenetic inheritance in plants and filamentous fungi. Science 293:1070-1074.
Martienssen, R. A., and Richards, E. J. 1995. DNA methylation in eukaryotes. Curr. Opin. Genet. Dev. 5:234-242.
Martinez-Zapater, J. M., Estelle, M. A., and Somerville, C. C. 1986. A highly repeated DNA sequence in *Arabidopsis thaliana*. Mol. Gen. Genet. 204:417-423.
Matzke, M. A., Mette, M. F., and Matzke, A. J. 2000. Transgene silencing by the host genome defense, implications for the evolution of epigenetic control mechanisms in plants and vertebrates. Plant Mol. Biol. 43:401-415.
Moscone, E. A., Matzke, M. A., and Matzke, A. J. 1996. The use of combined FISH/GISH in conjunction with DAPI counterstaining to identify chromosomes containing transgene inserts in amphidiploid tobacco. Chromosoma 105:231-236.
Nagar, S., Hanley-Bowdoin, L., and Robertson, D. 2002. Host DNA replication is induced by geminivirus infection of differentiated plant cells. Plant Cell 14:2995-3007.
Reichheld, J.-P., Sonobe, S., Clement, B., Chaubet, N., and Gigot, C. 1995. Cell cycle-regulated histone gene expression in synchronized plant cells. Plant J. 7:245-252.
Richards, E. J. 1997. DNA methylation and plant development. Trends Genet. 13:319-323.
Riou-Khamlichi, C., Huntley, R., Jacqmard, A., and Murray, J. A. 1999. Cytokinin activation of *Arabidopsis* cell division through a D-type cyclin. Science 283:1541-1544.
Ronemus, M. J., Galbiati, M., Ticknor, C., Chen, J., and Dellaporta, S. L. 1996. Demethylation-induced developmental pleiotropy in *Arabidopsis*. Science 273:654-657.
Saze, H., Scheid, O. M., and Paszkowski, J. 2003. Maintenance of CpG methylation is essential for epigenetic inheritance during plant gametogenesis. Nat. Genet. 34:65-69.
Soppe, W. J., Jacobsen, S. E., Alonso-Blanco, C., Jackson, J. P., Kakutani, T., Koornneef, M., and Peeters, A. J. 2000. The late flowering phenotype of fwa mutants is caused by gain-of-function epigenetic alleles of a homeodomain gene. Mol. Cell 6:791-802.
Soppe, W. J., Jasencakova, Z., Houben, A., Kakutani, T., Meister, A., Huang, M. S., Jacobsen, S. E., Schubert, I., and Fransz, P. F. 2002. DNA methylation controls histone H3 lysine 9 methylation and heterochromatin assembly in *Arabidopsis*. EMBO (Eur. Mol. Biol. Organ.) J. 21:6549-6559.
Steward, N., Ito, M., Yamaguchi, Y., Koizumi, N., and Sano, H. 2002. Periodic DNA methylation in maize nucleosomes and demethylation by environmental stress. J. Biol. Chem. 277:37741-37746.
Stokes, T. L., Kunkel, B. N., and Richards, E. J. 2002. Epigenetic variation in *Arabidopsis* disease resistance. Genes Dev. 16:171-182.
Stupar, R. M., Lilly, J. W., Town, C. D., Cheng, Z., Kaul, S., Buell, C. R., and Jiang, J. 2001. Complex mtDNA constitutes an approximate 620-kb insertion on *Arabidopsis thaliana* chromosome 2: Implication of potential sequencing errors caused by large-unit repeats. Proc. Natl. Acad. Sci. U.S.A. 98:5099-5103.
Tao, Y., Xie, Z., Chen, W., Glazebrook, J., Chang, H. S., Han, B., Zhu, T., Zou, G., and Katagiri, F. 2003. Quantitative nature of *Arabidopsis* responses during compatible and incompatible interactions with the bacterial pathogen Pseudomonas syringae. Plant Cell 15:317-330.
The Arabidopsis Genome Initiative. 2000. Analysis of the genome sequence of the flowering plant *Arabidopsis thaliana*. Nature 408:797-813.
Tompa, R., McCallum, C. M., Delrow, J., Henikoff, J. G., van Steensel, B., and Henikoff, S. 2002. Genome-wide profiling of DNA methylation reveals transposon targets of CHROMOMETHYLASE3. Curr. Biol. 12:65-68.
Tran, R. K., Henikoff, J, G., Zilberman. D., Ditt, R. F., Jacobsen, S. E., and Henikoff, S. 2005. DNA methylation profiling identifies CG methylation clusters in *Arabidopsis* genes. Curr. Biol. 15:154-159.
Vongs, A., Kakutani, T., Martienssen, R. A., and Richards, E. J. 1993. *Arabidopsis thaliana* DNA methylation mutants. Science 260:1926-1928.
Wada, Y., Miyamoto, K., Kusano, T., and Sano, H. 2004. Association between up-regulation of stress-responsive genes and hypomethylation of genomic DNA in tobacco plants. Mol. Genet. Genomics 271:658-666.
Wassenegger, M., Heimes, S., Riedel, L., and Sanger H. L. 1994. RNA-directed de novo methylation of genomic sequences in plants. Cell 76:567-576.
Weiss, A., Keshet, I., Razin, A., and Cedar, H. 1996. DNA demethylation in vitro: Involvement of RNA. Cell 86:709-718.
Whalen, M. C., Innes, R. W., Bent, A. F., and Staskawicz, B. J. 1991. Identification of *Pseudomonas syringae* pathogens of *Arabidopsis* and a bacterial locus determining avirulence on both *Arabidopsis* and soybean. Plant Cell 3:49-59.
Yoder, J. A., Walsh, C. P., and Bestor, T. H. 1997. Cytosine methylation and the ecology of intragenomic parasites. Trends Genet. 13:335-340.
Zhou, C., Zhang, L., Duan, J., Miki, B., and Wu, K. 2005. HISTONE DEACETYLASE19 is involved in jasmonic acid and ethylene signaling of pathogen response in *Arabidopsis*. Plant Cell 2005 17:1196-204
Zluvova, J., Janousek, B., and Vyskot, B. 2001. Immunohistochemical study of DNA methylation dynamics during plant development. J. Exp. Bot. 52:2265-2273.

AUTHOR-RECOMMENDED INTERNET RESOURCES

The Arabidopsis Information Resource (TAIR) database: www.Arabidopsis.org
The National Center for Biotechnology Information Gene Expression Omnibus website: www.ncbi.nlm.nih.gov/geo